IEICE TRANS. FUNDAMENTALS, VOL.E92–A, NO.3 MARCH 2009

PAPER Special Section on Latest Advances in Fundamental Theories of Signal Processing

Constraints of Second-Order Vanishing Moments on Lattice Structures for Non-separable Orthogonal Symmetric Wavelets

Atsuyuki ADACHI[†a)], ***Nonmember***, **Shogo MURAMATSU**[†], ***Member***, ***and*** **Hisakazu KIKUCHI**[†], ***Fellow***

SUMMARY In this paper, a design method of two-dimensional (2-D) orthogonal symmetric wavelets is proposed by using a lattice structure for multi-dimensional (M-D) linear-phase paraunitary filter banks (LPPUFB), which the authors have proposed as a previous work and then modified by Lu Gan et al. The derivation process for the constraints on the second-order vanishing moments is shown and some design examples obtained through optimization with the constraints are exemplified. In order to verify the significance of the constraints, some experimental results are shown for Lena and Barbara image.

key words: *wavelets, orthogonal transforms, non-separable filter banks, vanishing moments, video coding*

1. Introduction

Still picture codec standards, such as JPEG and JPEG2000, and motion picture codec standards, such as MPEG-1/2 and H.264/AVC, employ transform coding techniques as basic components for reducing spatial redundancy [1]–[3]. The coding performance of whole system is severely influenced by the choice of the transform.

JPEG and MPEG-1/2 consist of a 8×8 two-dimensional (2-D) discrete cosine transform (DCT). DCT is known as a quasi-optimal transform for the first-order autoregressive process with a correlation close to 1. As well, the transform kernel is defined by the cosine function and efficient computation is available through some fast algorithms. From these reasons, DCT has favourably been used in both of still and motion picture codecs. The independent block processing, however, makes block boundaries visible and the large basis images of high frequency components causes mosquito noise for very low bit-rates. JPEG2000 tries to solve these problems by introducing discrete wavelet transforms (DWTs). The DWTs contribute not only to gain coding performances and realize the spatial scalability, but also to reduce the blocking artifacts and the mosquito noise, because of their overlapping basis images and their different sizes suitable for different frequency components.

It is well known that there is no 1-D 2-channel filter bank which simultaneously satisfies all of the overlapping, linear-phase and paranunitary (i.e. orthogonal) property [4]. It is also true for separable 2-D 2×2-channel filter banks, which are employed in JPEG2000. Non-separable 2×2-channel filter banks, however, can simultaneously satisfy all of the previous properties. As well, image and video processing requires us to pay attention to frequency support of original signals because it may be non-separable [5]. From these backgrounds, M-D non-separable systems which simultaneously satisfy the orthogonal, overlapping and linear-phase property have been considered by several researches so far.

The authors also proposed non-separable transforms by using 2×2-channel linear-phase paraunitary filter banks (LPPUFBs) in the lattice structure as a previous work [6]. Furthermore, Lu Gan et al. showed the way of reducing the number of parameters to be optimized while preserving the class [7]. Since the orthogonal, overlapping, and linear-phase property are guaranteed, the lattice structure is convenient in terms of design and implementation. Additionally, we can construct 2×2-decomposition symmetric orthogonal DWTs by hierarchically applying the lattice structure. However, it has not been clarified how to design DWTs with vanishing moments through the lattice structure. Although Stanhill et al. exemplified a design procedure of such DWTs [8], [9], no constraint on design parameters in closed form has not been shown. For the 1-D case, the article [10] showed a design procedure of M-band orthogonal symmetric wavelets with lattice structures of second-order vanishing moments. In this work, it is shown that the constraints can be obtained in closed form of design parameters for the 2×2-channel 2-D lattice structure by using the similar approach to the 1-D lattice. Indeed, we design filter banks with our new method, and through an experiment on image coding, we verify the significance.

Organization of this paper is as follows: Section 2 reviews the design method of LPPUFBs based on lattice structure. Section 3 derives the constraints on the second-order vanishing moments for the lattice structure. Section 4 shows the results of the optimal design, followed by conclusions in Sect. 5.

2. Review of M-D Orthogonal Symmetric DWTs

In this section, we review M-D LPPUFBs based on a lattice structure, which the authors have proposed as a previous work and then Lu Gan et al. improved. Then, orthogonal symmetric non-separable DWTs are summarized.

It is well known that there is no 1-D 2-channel filter bank which simultaneously satisfies the overlapping, linear-phase and paranunitary (i.e. orthogonal) property [4]. This limitation is taken over by 2-D 2×2-channel filter banks.

Manuscript received July 4, 2008.
Manuscript revised October 19, 2008.

[†]The authors are with the Faculty of Engineering, Niigata University, Niigata-shi, 950-2181 Japan.
a) E-mail: adatsu@telecom0.eng.niigata-u.ac.jp

DOI: 10.1587/transfun.E92.A.788

Non-separable systems, however, allow us to design 2×2-channel LPPUFBs with over lapping bases, which can simultaneously decompose a picture into vertical and horizontal directions [6], [7], [9].

As a previous work, we have proposed a design procedure of M-D LPPUFBs based on a lattice structure [6]. Furthermore, Lu Gan et al. showed the way of reducing the number of parameters to be optimized while preserving the class [7]. Figure 1 shows a parallel structure of 2×2-channel filter banks, where $\downarrow \mathbf{M}$ and $\uparrow \mathbf{M}$ are respectively the downsampler and upsampler with factor $\mathbf{M} = \left(\begin{smallmatrix} 2 & 0 \\ 0 & 2 \end{smallmatrix}\right)$. $H_{k\ell}(\mathbf{z})$ and $F_{k\ell}(\mathbf{z})$ are respectively 2-D non-separable analysis and synthesis filters. A lattice structure of the analysis part of 2×2-channel LPPUFBs is given in Fig. 2, where $X(\mathbf{z})$ is input signal, $Y_k(\mathbf{z})$ is the k-th subband signal, z_d is the delay element of d-th dimension, $\mathbf{U}_0^{\{\emptyset\}}$ and $\mathbf{W}_n^{\{d\}}$ are arbitrary 2×2-decomposition orthogonal matrices, and K is a scaling factor given by $K = 2^{-(N_0+N_1)}$. From the paraunitary property, the impulse responses of synthesis filters $F_{k\ell}(\mathbf{z})$ are given as the 180°-rotated version of the counterpart analysis filters $H_{k\ell}(\mathbf{z})$.

A polyphase matrix of a 2×2-channel LPPUFB is given by

$$\mathbf{E}(z_0, z_1) = \left(\prod_{n_1=1}^{N_1} \mathbf{R}_{n_1}^{\{1\}} \mathbf{Q}(z_1)\right)\left(\prod_{n_0=1}^{N_0} \mathbf{R}_{n_0}^{\{0\}} \mathbf{Q}(z_0)\right) \mathbf{R}_0^{\{\emptyset\}} \mathbf{E}_0, \tag{1}$$

where $\prod_{n=1}^{N} \mathbf{A}_n = \mathbf{A}_N \mathbf{A}_{N-1} \cdots \mathbf{A}_2 \mathbf{A}_1$, and

$$\mathbf{R}_n^{\{d\}} = \begin{cases} \begin{pmatrix} \mathbf{W}_n^{\{d\}} & \mathbf{O}_2 \\ \mathbf{O}_2 & \mathbf{I}_2 \end{pmatrix}, & d \in \{0, 1\} \\ \begin{pmatrix} \mathbf{W}_n^{\{\emptyset\}} & \mathbf{O} \\ \mathbf{O} & \mathbf{U}_n^{\{\emptyset\}} \end{pmatrix}, & d = \emptyset \end{cases}, \tag{2}$$

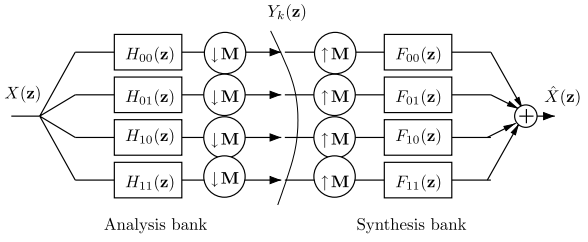

Fig. 1 Parallel structure of 2×2-channel LPPUFB.

$$\mathbf{Q}(z) = \frac{1}{2}\begin{pmatrix} \mathbf{I}_2 & \mathbf{I}_2 \\ \mathbf{I}_2 & -\mathbf{I}_2 \end{pmatrix}\begin{pmatrix} \mathbf{I}_2 & \mathbf{O}_2 \\ \mathbf{O}_2 & z^{-1}\mathbf{I}_2 \end{pmatrix}\begin{pmatrix} \mathbf{I}_2 & \mathbf{I}_2 \\ \mathbf{I}_2 & -\mathbf{I}_2 \end{pmatrix}, \tag{3}$$

$$\mathbf{E}_0 = \frac{1}{2}\begin{pmatrix} 1 & 1 & 1 & 1 \\ 1 & -1 & -1 & 1 \\ 1 & 1 & -1 & -1 \\ 1 & -1 & 1 & -1 \end{pmatrix}. \tag{4}$$

$\mathbf{I}_N$ and $\mathbf{O}_N$ denote the $N \times N$ identity and null matrices, respectively.

Controlling $\mathbf{W}_n^{\{d\}}$ and $\mathbf{U}_0^{\{\emptyset\}}$, enables us to design filter banks which can have various characteristics, while guaranteeing the orthogonal and symmetric property [6], [7]. The resulting filters in the system will have $2(N_0 + 1) \times 2(N_1 + 1)$ taps.

Our transform can construct the same multiresolution analysis as one given by separable systems with 1-D 2-channel filter banks. While the conventional 5/3 and 9/7 DWTs are biorthogonal transforms, our DWTs satisfy the orthogonality, as well as the symmetric and overlapping property.

3. Derivation of Constraints on the 2nd-Order Vanishing Moments

In this section, we derive the constraints on the second-order vanishing moments for the lattice structure.

3.1 Vanishing Moments of the 2-D DWTs

The article [8] describes the condition of vanishing moments of 2-D non-separable DWTs.

The condition of the first-order vanishing moments is given by

$$H_{00}(z_0, z_1)\big|_{\left(\begin{smallmatrix} z_0 \\ z_1 \end{smallmatrix}\right) \in \left\{\left(\begin{smallmatrix} 1 \\ -1 \end{smallmatrix}\right), \left(\begin{smallmatrix} -1 \\ 1 \end{smallmatrix}\right), \left(\begin{smallmatrix} -1 \\ -1 \end{smallmatrix}\right)\right\}} = 0 \tag{5}$$

and, that of the second-order vanishing moments is given by

$$\frac{\partial}{\partial z_d} H_{00}(z_0, z_1)\Big|_{\left(\begin{smallmatrix} z_0 \\ z_1 \end{smallmatrix}\right) \in \left\{\left(\begin{smallmatrix} 1 \\ -1 \end{smallmatrix}\right), \left(\begin{smallmatrix} -1 \\ 1 \end{smallmatrix}\right), \left(\begin{smallmatrix} -1 \\ -1 \end{smallmatrix}\right)\right\}} = 0, \quad d \in \{0, 1\}. \tag{6}$$

The article [9] shows a design example of 2-D orthogonal symmetric DWTs with maximum vanishing moments.

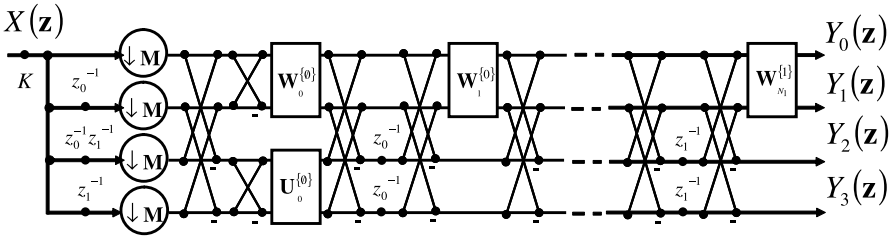

Fig. 2 Lattice structure of 2×2-channel LPPUFB (analysis bank), where $\mathbf{M} = \left(\begin{smallmatrix} 2 & 0 \\ 0 & 2 \end{smallmatrix}\right)$, K is a scalling factor, $\mathbf{U}_0^{\{\emptyset\}}$ and $\mathbf{W}_n^{\{d\}}$ are orthogonal matrices.

The design parameters, however, are not constrained directly and, thus it was difficult to design the filters systematically. The article [10] shows a design method of a lattice structure for 1-D M-channel LPPUFBs with the second-order vanishing moments. In this work, by using the similar approach, we consider constraints of the second-order vanishing moments imposed for constructing 2-D LPPUFBs.

3.2 Constraints for 2-D Non-separable Lattice Structure

In the lattice structure shown in Fig. 2, the constraints on the first-order vanishing moments in Eq. (5) is rewritten in terms of the design parameters by

$$\mathbf{W}_0^{\{\emptyset\}T} = \left(\prod_{n_1=1}^{N_1} \mathbf{W}_{n_1}^{\{1\}}\right) \cdot \left(\prod_{n_0=1}^{N_0} \mathbf{W}_{n_0}^{\{1\}}\right) \tag{7}$$

[6]. As well, the constraints on the second-order vanishing moments are derived by

$$\mathbf{C}_0^T \begin{pmatrix}1\\0\end{pmatrix} + \frac{1}{2}\begin{pmatrix}0\\1\end{pmatrix} = \begin{pmatrix}0\\0\end{pmatrix}, \tag{8}$$

$$\mathbf{C}_1^T \begin{pmatrix}1\\0\end{pmatrix} + \frac{1}{2}\begin{pmatrix}1\\0\end{pmatrix} = \begin{pmatrix}0\\0\end{pmatrix}, \tag{9}$$

where

$$\mathbf{C}_0 = \left(\prod_{n_1=1}^{N_1} \mathbf{W}_{n_1}^{\{1\}}\right) \cdot \sum_{k_0=1}^{N_0} \left(\prod_{n_0=k_0}^{N_0} \mathbf{W}_{n_0}^{\{0\}}\right) \cdot \mathbf{U}_0^{\{\emptyset\}}, \tag{10}$$

$$\mathbf{C}_1 = \sum_{k_1=1}^{N_1} \left(\prod_{n_1=k_1}^{N_1} \mathbf{W}_{n_1}^{\{1\}}\right) \cdot \mathbf{U}_0^{\{\emptyset\}}. \tag{11}$$

The above constraints are newly derived in this paper. In the following section, let us detail the derivation.

3.3 Derivation of Constraints on the 2nd-Order Vanishing Moments

In order to show the derivation process of the constraints in Eqs. (8)–(11), let us begin with represent the lowpass filter $H_{00}(z_0, z_1)$ in terms of the poly-phase matrix $\mathbf{E}(z_0, z_1)$. Then, we obtain

$$\begin{aligned} H_{00}(z_0, z_1) &= \begin{pmatrix}1 & 0 & 0 & 0\end{pmatrix} \mathbf{E}(z_0^2, z_1^2)\mathbf{d}(z_0, z_1) \\ &= \begin{pmatrix}1 & 0 & 0 & 0\end{pmatrix} \left(\prod_{n_1=1}^{N_1} \mathbf{R}_{n_1}^{\{1\}} \mathbf{Q}(z_1^2)\right) \\ &\quad \times \left(\prod_{n_0=1}^{N_0} \mathbf{R}_{n_0}^{\{0\}} \mathbf{Q}(z_0^2)\right) \mathbf{R}_0^{\{\emptyset\}} \mathbf{E}_0 \mathbf{d}(z_0, z_1), \end{aligned} \tag{12}$$

where

$$\mathbf{d}(z_0, z_1) = \begin{pmatrix} 1 \\ z_0^{-1} \\ z_1^{-1} \\ z_0^{-1} z_1^{-1} \end{pmatrix}.$$

As well, the partial derivatives with respect to each variable are given by

$$\begin{aligned} &\frac{\partial}{\partial z_0} H_{00}(z_0, z_1) \\ &= \begin{pmatrix}1 & 0 & 0 & 0\end{pmatrix} \left(\prod_{n_1=1}^{N_1} \mathbf{R}_{n_1}^{\{1\}} \mathbf{Q}(z_1^2)\right) \\ &\quad \times \left\{ \sum_{k_0=1}^{N_0} \left(\prod_{n_0=1}^{N_0} \mathbf{R}_{n_0}^{\{0\}} \frac{\partial^{\delta[n_0-k_0]}}{\partial z_0^{\delta[n_0-k_0]}} \mathbf{Q}(z_0^2) \right) \right\} \\ &\quad \times \mathbf{R}_0^{\{\emptyset\}} \mathbf{E}_0 \mathbf{d}(z_0, z_1) \\ &\quad + \begin{pmatrix}1 & 0 & 0 & 0\end{pmatrix} \left(\prod_{n_1=1}^{N_1} \mathbf{R}_{n_1}^{\{1\}} \mathbf{Q}(z_1^2)\right) \\ &\quad \times \left(\prod_{n_0=1}^{N_0} \mathbf{R}_{n_0}^{\{0\}} \mathbf{Q}(z_0^2)\right) \mathbf{R}_0^{\{\emptyset\}} \mathbf{E}_0 \frac{\partial}{\partial z_0} \mathbf{d}(z_0, z_1), \end{aligned} \tag{13}$$

$$\begin{aligned} &\frac{\partial}{\partial z_1} H_{00}(z_0, z_1) \\ &= \begin{pmatrix}1 & 0 & 0 & 0\end{pmatrix} \\ &\quad \times \left\{ \sum_{k_1=1}^{N_1} \left(\prod_{n_1=1}^{N_1} \mathbf{R}_{n_1}^{\{1\}} \frac{\partial^{\delta[n_1-k_1]}}{\partial z_1^{\delta[n_1-k_1]}} \mathbf{Q}(z_1^2) \right) \right\} \\ &\quad \times \left(\prod_{n_0=1}^{N_0} \mathbf{R}_{n_0}^{\{0\}} \mathbf{Q}(z_0^2)\right) \mathbf{R}_0^{\{\emptyset\}} \mathbf{E}_0 \mathbf{d}(z_0, z_1) \\ &\quad + \begin{pmatrix}1 & 0 & 0 & 0\end{pmatrix} \left(\prod_{n_1=1}^{N_1} \mathbf{R}_{n_1}^{\{1\}} \mathbf{Q}(z_1^2)\right) \\ &\quad \times \left(\prod_{n_0=1}^{N_0} \mathbf{R}_{n_0}^{\{0\}} \mathbf{Q}(z_0^2)\right) \mathbf{R}_0^{\{\emptyset\}} \mathbf{E}_0 \frac{\partial}{\partial z_1} \mathbf{d}(z_0, z_1) \end{aligned} \tag{14}$$

respectively, where $\delta[n]$ is the sequence which equals one when $n = 0$, and zero otherwise.

Let $\zeta_d \in \{-1, 1\}$. Substituting $z_d = \zeta_d$, we can simplify Eqs. (13) and (14) to

$$\begin{aligned} &\frac{\partial}{\partial z_0} H_{00}(z_0, z_1)\Big|_{\binom{z_0}{z_1}=\binom{\zeta_0}{\zeta_1}} \\ &\quad = -\zeta_0 \begin{pmatrix}1 & 0\end{pmatrix} \begin{pmatrix}N_0\mathbf{I} & -\mathbf{C}_0\end{pmatrix} \mathbf{E}_0 \mathbf{d}(\zeta_0, \zeta_1) - \frac{1}{2}\zeta_0^2(1 + \zeta_1), \end{aligned} \tag{15}$$

$$\begin{aligned} &\frac{\partial}{\partial z_1} H_{00}(z_0, z_1)\Big|_{\binom{z_0}{z_1}=\binom{\zeta_0}{\zeta_1}} \\ &\quad = -\zeta_1 \begin{pmatrix}1 & 0\end{pmatrix} \begin{pmatrix}N_1\mathbf{I} & -\mathbf{C}_1\end{pmatrix} \mathbf{E}_0 \mathbf{d}(\zeta_0, \zeta_1) - \frac{1}{2}\zeta_1^2(1 + \zeta_0), \end{aligned} \tag{16}$$

respectively, where we used some properties shown in Appendix A and the constraint of the first-order vanishing moments in Eq. (7) for simplifying the second term in the right-hand side.

Finally, using the following relations:

$$\mathbf{E}_0\mathbf{d}(1,-1) = 2\begin{pmatrix}0 & 0 & 1 & 0\end{pmatrix}^T,$$
$$\mathbf{E}_0\mathbf{d}(-1,1) = 2\begin{pmatrix}0 & 0 & 0 & 1\end{pmatrix}^T,$$
$$\mathbf{E}_0\mathbf{d}(-1,-1) = 2\begin{pmatrix}0 & 1 & 0 & 0\end{pmatrix}^T,$$

the condition in Eq. (6) is reduced to

$$\begin{pmatrix}1 & 0\end{pmatrix}\mathbf{C}_0\begin{pmatrix}1\\0\end{pmatrix} = 0, \tag{17}$$
$$\begin{pmatrix}1 & 0\end{pmatrix}\mathbf{C}_0\begin{pmatrix}0\\1\end{pmatrix} + \frac{1}{2} = 0, \tag{18}$$
$$\begin{pmatrix}1 & 0\end{pmatrix}\mathbf{C}_1\begin{pmatrix}1\\0\end{pmatrix} + \frac{1}{2} = 0, \tag{19}$$
$$\begin{pmatrix}1 & 0\end{pmatrix}\mathbf{C}_1\begin{pmatrix}0\\1\end{pmatrix} = 0. \tag{20}$$

Expressing the above relations together, the constraints in Eqs. (8) and (9) are given.

3.4 Number of Control Parameters

The number of parameters are discussed in the followings. The polyphase matrix of order (N_0, N_1) is composed of $N_0 + N_1 + 2$ orthonormal matrices of size 2×2. Thus, the total number of control parameters are $N_0 + N_1 + 2$ in the form of rotation angles. Let us see how the second-order vanishing moment constraints reduce the number of design parameters and the number becomes $N_0 + N_1 - 3$. Our discussion here temporally restricts for all orthonormal matrices to be in the following rotation form:

$$\mathbf{T}[\theta] = \begin{pmatrix}\cos\theta & -\sin\theta\\ \sin\theta & \cos\theta\end{pmatrix}. \tag{21}$$

3.4.1 Triangle Analysis [10]

Let $\mathbf{a} = (1, 0)^T$ and $\mathbf{o} = (0, 0)^T$. Then, Eqs. (8) and (9) can be rewritten as follows:

$$\mathbf{a}_d + \sum_{k_d=1}^{N_d-1}\prod_{n_d=1}^{N_d-k_d}\mathbf{W}_{n_d}^{\{d\}}\mathbf{a}_d + \frac{1}{2}\mathbf{U}_0^{\{\emptyset\}}\mathbf{V}^{\{d\}}\mathbf{W}_2^{\{d\}}\mathbf{W}_1^{\{d\}}\mathbf{a}_d = \mathbf{o},\ d \in (0,1), \tag{22}$$

where

$$\mathbf{a}_0 = \left(\prod_{n_0=1}^{N_0}\mathbf{W}_{n_0}^{\{0\}}\right)^T\left(\prod_{n_1=1}^{N_1}\mathbf{W}_{n_1}^{\{1\}}\right)^T\mathbf{a}, \tag{23}$$
$$\mathbf{a}_1 = \left(\prod_{n_1=1}^{N_1}\mathbf{W}_{n_1}^{\{1\}}\right)^T\mathbf{a}, \tag{24}$$
$$\mathbf{V}^{\{0\}} = \begin{cases}\mathbf{T}\left[\frac{\pi}{2}\right]\prod_{n_1=1}^{N_1}\mathbf{W}_{n_1}^{\{1\}}, & N_0 \le 2\\ \mathbf{T}\left[\frac{\pi}{2}\right]\prod_{n_1=1}^{N_1}\mathbf{W}_{n_1}^{\{1\}}\prod_{n_0=3}^{N_0}\mathbf{W}_{n_0}^{\{0\}}, & N_0 > 2\end{cases}, \tag{25}$$
$$\mathbf{V}^{\{1\}} = \begin{cases}\mathbf{I}, & N_1 \le 2,\\ \prod_{n_1=3}^{N_1}\mathbf{W}_{n_1}^{\{1\}}, & N_1 > 2\end{cases}. \tag{26}$$

Note that $\|\mathbf{a}_0\| = \|\mathbf{a}_1\| = \|\mathbf{a}\| = 1$ since $\mathbf{W}_{n_d}^{\{d\}}$ are all orthonormal. Equation (22) enables us to make a similar discussion to the article [10] with regard to the second-order vanishing moment conditions.

It is verified that Eq. (22) never hold for $N_0, N_1 < 2$ from the vector lengths [10]. Thus, the filter sizes should be more than $2(N_0 + 1) \times 2(N_1 + 1) = 6 \times 6$.

3.4.2 Example of Minimal Support Case

For minimal support case, i.e. $N_0 = N_1 = 2$, we have three vectors $\mathbf{x}_1^{\{d\}} = \mathbf{a}_d$, $\mathbf{x}_2^{\{d\}} = \mathbf{W}_1^{\{d\}}\mathbf{x}_1^{\{d\}}$ and $\mathbf{x}_3^{\{d\}} = \mathbf{U}_0^{\{\emptyset\}}\mathbf{V}^{\{d\}}\mathbf{W}_2^{\{d\}}\mathbf{x}_2^{\{d\}}/2$ in Eq. (22) for each $d \in \{0, 1\}$, where $\|\mathbf{x}_1^{\{d\}}\| = \|\mathbf{x}_2^{\{d\}}\| = 1$ and $\|\mathbf{x}_3^{\{d\}}\| = 1/2$. These vectors should constitute a bilateral triangle. The rotation angles from $\mathbf{x}_1^{\{d\}}$ to $\mathbf{x}_2^{\{d\}}$ and from $\mathbf{x}_2^{\{d\}}$ to $\mathbf{x}_3^{\{d\}}$ are respectively given as follows:

$$\begin{aligned}\theta_{1\to2}^{\{d\}} &= (-1)^{\sigma_d}\left\{\pi - 2\sin^{-1}\left(\frac{\|\mathbf{x}_3^{\{d\}}\|}{2\|\mathbf{x}_1^{\{d\}}\|}\right)\right\}\\ &= (-1)^{\sigma_d}\left\{\pi - 2\sin^{-1}\left(\frac{1}{4}\right)\right\},\\ \theta_{2\to3}^{\{d\}} &= (-1)^{\sigma_d}\left\{\pi - \cos^{-1}\left(\frac{\|\mathbf{x}_3^{\{d\}}\|}{2\|\mathbf{x}_1^{\{d\}}\|}\right)\right\}\\ &= (-1)^{\sigma_d}\left\{\pi - \cos^{-1}\left(\frac{1}{4}\right)\right\},\end{aligned}$$

where $\sigma_d \in (0, 1)$ is the sign, which controls the rotational direction.

Thus, matrices $\mathbf{W}_1^{\{0\}}$ and $\mathbf{W}_1^{\{1\}}$ are determined as

$$\mathbf{W}_1^{\{d\}} = \mathbf{T}\left[\theta_{1\to2}^{\{d\}}\right],\ d \in (0,1). \tag{27}$$

From the relation $\mathbf{x}_3^{\{d\}} = \|\mathbf{x}_3^{\{d\}}\|\mathbf{T}[\theta_{2\to3}^{\{d\}}]\mathbf{x}_2^{\{d\}}$, we see that $\mathbf{W}_2^{\{d\}}$ is also imposed the following condition:

$$\mathbf{W}_2^{\{d\}} = \mathbf{V}^{\{d\}T}\mathbf{U}_0^{\{\emptyset\}T}\mathbf{T}\left[\theta_{2\to3}^{\{d\}}\right],\ d \in (0,1). \tag{28}$$

Since $\mathbf{V}^{\{1\}} = \mathbf{I}$ and $\mathbf{V}^{\{0\}} = \mathbf{T}[\pi/2]\mathbf{W}_2^{\{1\}}\mathbf{W}_1^{\{1\}}$, $\mathbf{W}_2^{\{1\}}$ and $\mathbf{W}_2^{\{1\}}$ are determined in the following order:

$$\mathbf{W}_2^{\{1\}} = \mathbf{U}_0^{\{\emptyset\}T}\mathbf{T}\left[\theta_{2\to3}^{\{1\}}\right], \tag{29}$$
$$\mathbf{W}_2^{\{0\}} = \mathbf{W}_1^{\{1\}T}\mathbf{W}_2^{\{1\}T}\mathbf{T}\left[\frac{\pi}{2}\right]^T\mathbf{U}_0^{\{\emptyset\}T}\mathbf{T}\left[\theta_{2\to3}^{\{0\}}\right]. \tag{30}$$

Note that $\mathbf{W}_0^{\{\emptyset\}}$ is fixed for the first-order vanishing moment. Therefore, we are allowed to control only $\mathbf{U}_0^{\{\emptyset\}}$.

3.4.3 Case for $N_0, N_1 > 2$

For $N_0, N_1 > 2$, Eq. (22) can be seen as a triangle consisting

of the three vectors defined by

$$\mathbf{x}_1^{\{d\}} = \mathbf{a}_d, \tag{31}$$

$$\mathbf{x}_2^{\{d\}} = \mathbf{W}_1^{\{d\}}\mathbf{x}_1^{\{d\}}, \tag{32}$$

and

$$\begin{aligned}\mathbf{x}_3^{\{d\}} &= \left(\mathbf{I} + \sum_{k_d=1}^{N_d-3}\prod_{n_d=3}^{N_d-k_d}\mathbf{W}_{n_d}^{\{d\}} + \frac{1}{2}\mathbf{U}_0^{\{\emptyset\}}\mathbf{V}^{\{d\}}\right)\mathbf{W}_2^{\{d\}}\mathbf{x}_2^{\{d\}} \\ &= \mathbf{W}_2^{\{d\}}\left(\mathbf{I} + \sum_{k_d=1}^{N_d-3}\prod_{n_d=3}^{N_d-k_d}\mathbf{W}_{n_d}^{\{d\}} + \frac{1}{2}\mathbf{U}_0^{\{\emptyset\}}\mathbf{V}^{\{d\}}\right)\mathbf{x}_2^{\{d\}}. \end{aligned} \tag{33}$$

The last equation uses the fact that the adopted orthonormal matrices are all in the form in Eq. (21).

The length of vector $\mathbf{x}_3^{\{d\}}$ varies and is given by

$$\|\mathbf{x}_3^{\{d\}}\| = \left\|\left(\mathbf{I} + \sum_{k_d=1}^{N_d-3}\prod_{n_d=3}^{N_d-k_d}\mathbf{W}_{n_d}^{\{d\}} + \frac{1}{2}\mathbf{U}_0^{\{\emptyset\}}\mathbf{V}^{\{d\}}\right)\mathbf{a}\right\|, \tag{34}$$

where we used the fact that $\mathbf{x}_2^{\{d\}}$ is a rotation of $\mathbf{a}$. Equivalently, we have

$$\|\mathbf{x}_3^{\{d\}}\| = \sqrt{c_d(\Theta)^2 + s_d(\Theta)^2}, \tag{35}$$

where Θ is a set of the rotation angle parameters and

$$c_d(\Theta) = 1 + \sum_{k_d=1}^{N_d-3}\cos\left(\sum_{n_d=3}^{N_d-k_d}\theta_{n_d}^{\{d\}}\right) + \frac{1}{2}\cos\left(\theta_{\mathrm{U}}^{\{\emptyset\}} + \theta_{\mathrm{V}}^{\{d\}}\right), \tag{36}$$

$$s_d(\Theta) = \sum_{k_d=1}^{N_d-3}\sin\left(\sum_{n_d=3}^{N_d-k_d}\theta_{n_d}^{\{d\}}\right) + \frac{1}{2}\sin\left(\theta_{\mathrm{U}}^{\{\emptyset\}} + \theta_{\mathrm{V}}^{\{d\}}\right), \tag{37}$$

where $\theta_{n_d}^{\{d\}}$ and $\theta_{\mathrm{U}}^{\{\emptyset\}}$ are the rotation angles of matrices $\mathbf{W}_{n_d}^{\{d\}}$ and $\mathbf{U}_0^{\{\emptyset\}}$, respectively. We also define

$$\begin{aligned}\theta_{\mathrm{V}}^{\{1\}} &= \sum_{n_1=3}^{N_1}\theta_{n_1}^{\{1\}} \\ \theta_{\mathrm{V}}^{\{0\}} &= \frac{\pi}{2} + \sum_{n_1=1}^{N_1}\theta_{n_1}^{\{1\}} + \sum_{n_0=3}^{N_0}\theta_{n_0}^{\{0\}}.\end{aligned}$$

Note that $\|\mathbf{x}_3^{\{d\}}\|$ is independent of the choice of $\mathbf{W}_1^{\{d\}}$ and $\mathbf{W}_2^{\{d\}}$, which will be fixed later.

It here should be noted that the length of vector $\mathbf{x}_3^{\{d\}}$ must satisfy the following triangle inequality:

$$0 \le \|\mathbf{x}_3^{\{d\}}\| \le \|\mathbf{x}_1^{\{d\}}\| + \|\mathbf{x}_2^{\{d\}}\| = 2. \tag{38}$$

For $N_d = 3$, this condition is always satisfied with $\|\mathbf{x}_3^{\{d\}}\| \le 3/2$, whereas the free parameters should be constrained to hold this condition for $N_d > 3$ [10].

Let $\mathbf{U}_0^{\{\emptyset\}}$ and $\mathbf{W}_{n_d}^{\{d\}}$ for $n_d = 3, 4, \cdots, N_d$, $d \in (0, 1)$ be free to be chosen. The design process starts to calculate the length $\|\mathbf{x}_3^{\{1\}}\|$ for direction $d = 1$ then proceed to direction $d = 0$ after the process for $d = 1$ is done. Provided the condition in Eq. (38) holds, we can solve the rotation angles among the vectors as

$$\begin{aligned}\theta_{1\to2}^{\{d\}} &= (-1)^{\sigma_d}\left\{\pi - 2\sin^{-1}\left(\|\mathbf{x}_3^{\{d\}}\|/2\right)\right\}, \\ \theta_{2\to3}^{\{d\}} &= (-1)^{\sigma_d}\left\{\pi - \cos^{-1}\left(\|\mathbf{x}_3^{\{d\}}\|/2\right)\right\}.\end{aligned}$$

From Eqs. (31) and (32), matrix $\mathbf{W}_1^{\{d\}}$ is fixed as

$$\mathbf{W}_1^{\{d\}} = \mathbf{T}\left[\theta_{1\to2}^{\{d\}}\right],\ d \in (0, 1). \tag{39}$$

Thus, the number of free parameters is reduced.

From the relation $\mathbf{x}_3^{\{d\}} = \|\mathbf{x}_3^{\{d\}}\|\mathbf{T}[\theta_{2\to3}^{\{d\}}]\mathbf{x}_2^{\{d\}}$ with Eq. (32), we have

$$\begin{aligned}\mathbf{W}_2^{\{d\}} = \frac{1}{\|\mathbf{x}_3^{\{d\}}\|} &\times \left\{\mathbf{I} + \sum_{k_d=1}^{N_d-3}\prod_{n_d=3}^{N_d-k_d}\mathbf{W}_{n_d}^{\{d\}} + \frac{1}{2}\mathbf{U}_0^{\{\emptyset\}}\mathbf{V}^{\{d\}}\right\}^T \mathbf{T}\left[\theta_{2\to3}^{\{d\}}\right], \\ &d \in (0, 1),\end{aligned} \tag{40}$$

or equivalently

$$\theta_2^{\{d\}} = -\tan^{-1}\frac{s_d(\Theta)}{c_d(\Theta)} + \theta_{2\to3},\ d \in (0, 1), \tag{41}$$

where we used the fact that a linear combination of rotation matrices is represented by a scaled rotation matrix. Although $\|\mathbf{x}_3^{\{0\}}\|$ depends on matrices $\mathbf{W}_1^{\{1\}}$ and $\mathbf{W}_2^{\{1\}}$, it is solvable after the process for $d = 1$.

In summary, the first-order vanishing moment constraint in Eq. (7) reduces one parameter since matrix $\mathbf{W}_0^{\{d\}}$ depends on other matrices, where the angle $\theta_{\mathrm{W}}^{\{\emptyset\}}$ is imposed to be $\theta_{\mathrm{W}}^{\{\emptyset\}} = -\sum_{d\in(0,1)}\sum_{n_d=1}^{N_d}\theta_{\mathrm{n_d}}^{\{d\}}$. Additionally, the second-order vanishing moment constraint reduces four parameters for matrices $\mathbf{W}_1^{\{1\}}$, $\mathbf{W}_2^{\{1\}}$, $\mathbf{W}_1^{\{0\}}$ and $\mathbf{W}_2^{\{0\}}$. In total, the number of parameters to be freely chosen results in $N_0 + N_1 - 3$. For $N_0, N_1 > 3$, however, we have to take special care of the lengths of vectors $\mathbf{x}_3^{\{0\}}$ and $\mathbf{x}_3^{\{1\}}$. They must be constrained to be shorter than two. Under this constraint, we are allowed to control $\mathbf{U}_0^{\{\emptyset\}}$ and $\mathbf{W}_{n_d}^{\{d\}}$ for $n_d = 3, 4, \cdots, N_d$, $d \in (0, 1)$.

3.5 Alternative Parameterization with Flipping

The previous discussion restricts all controllable matrices to be in the rotation form. Experimentally, other forms of parameterization is often favorable. We here briefly summarize an alternative parameterization.

It is allowed to rewrite $\mathbf{V}_0^{\{0\}}$ for $N_0 \ge 2$ in Eq. (25) as

$$\mathbf{V}^{\{0\}} = \mathbf{J}\prod_{n_1=1}^{N_1}\mathbf{W}_{n_1}^{\{1\}}\prod_{n_0=3}^{N_0}\mathbf{W}_{n_0}^{\{0\}}, \tag{42}$$

where $\mathbf{J}$ is the 2×2 counter identity matrix, i.e. $\left(\begin{smallmatrix}0 & 1\\ 1 & 0\end{smallmatrix}\right)$, and used instead of $\mathbf{T}[\pi/2]$. Note that matrix $\mathbf{J}$ is orthonormal, but not rotational as in Eq. (21).

Let us parameterize $\mathbf{W}_{N_d}^{\{d\}}$ as $\mathbf{J}\overline{\mathbf{W}}_{N_d}^{\{d\}}$ with a rotation matrix $\overline{\mathbf{W}}_{N_d}^{\{d\}}$. Then, we can modify Eqs. (25) and (26) as

$$\mathbf{V}^{\{1\}} = \mathbf{J}\overline{\mathbf{W}}_{N_1}^{\{1\}} \prod_{n_1=3}^{N_1-1} \mathbf{W}_{n_1}^{\{1\}},$$

$$\begin{aligned}\mathbf{V}^{\{0\}} &= \mathbf{J}^2\overline{\mathbf{W}}_{N_1}^{\{1\}} \prod_{n_1=1}^{N_1-1} \mathbf{W}_{n_1}^{\{1\}} \mathbf{J}\overline{\mathbf{W}}_{N_0}^{\{0\}} \prod_{n_0=3}^{N_0-1} \mathbf{W}_{n_0}^{\{0\}} \\ &= \mathbf{J}\left(\overline{\mathbf{W}}_{N_1}^{\{1\}} \prod_{n_1=1}^{N_1-1} \mathbf{W}_{n_1}^{\{1\}}\right)^T \overline{\mathbf{W}}_{N_0}^{\{0\}} \prod_{n_0=3}^{N_0-1} \mathbf{W}_{n_0}^{\{0\}},\end{aligned}$$

where the relation $\mathbf{JT}[\theta]\mathbf{J} = \mathbf{T}[\theta]^T$ is used.

It is easy to see that if $\mathbf{U}_0^{\{\emptyset\}}$ is parameterized as $\overline{\mathbf{U}}_0^{\{\emptyset\}}\mathbf{J}$ with a rotation matrix $\overline{\mathbf{U}}_0^{\{\emptyset\}}$, matrix $\mathbf{J}$ vanishes from Eq. (33). As a result, the same discussion follows as the previous subsection, except that $\theta_{\mathrm{U}}^{\{\emptyset\}} + \theta_{\mathrm{V}}^{\{d\}}$ in Eqs. (36) and (37) is given by

$$\theta_{\mathrm{U}}^{\{\emptyset\}} + \theta_{\mathrm{V}}^{\{1\}} = \overline{\theta}_{\mathrm{U}}^{\{\emptyset\}} + \overline{\theta}_{N_1}^{\{1\}} + \sum_{n_1=3}^{N_1-1} \theta_{n_1}^{\{1\}},$$

$$\theta_{\mathrm{U}}^{\{\emptyset\}} + \theta_{\mathrm{V}}^{\{0\}} = \overline{\theta}_{\mathrm{U}}^{\{\emptyset\}} - \left(\overline{\theta}_{N_1}^{\{1\}} + \sum_{n_1=1}^{N_1-1} \theta_{n_1}^{\{1\}}\right) + \overline{\theta}_{N_0}^{\{0\}} + \sum_{n_0=3}^{N_0-1} \theta_{n_0}^{\{0\}},$$

where $\overline{\theta}_{\mathrm{U}}^{\{\emptyset\}}$, $\overline{\theta}_{N_0}^{\{0\}}$ and $\overline{\theta}_{N_1}^{\{1\}}$, are the rotation angles of matrices $\overline{\mathbf{U}}_0^{\{\emptyset\}}$. $\overline{\mathbf{W}}_{N_0}^{\{0\}}$. and $\overline{\mathbf{W}}_{N_1}^{\{1\}}$, respectively. Note that the first-order vanishing moment imposes the angle $\theta_{\mathrm{W}}^{\{\emptyset\}}$ of matrix $\mathbf{W}_0^{\{\emptyset\}}$ to be $\theta_{\mathrm{W}}^{\{\emptyset\}} = \left(\overline{\theta}_{\mathrm{N_1}}^{\{1\}} + \sum_{n_1=1}^{N_1-1} \theta_{\mathrm{n_1}}^{\{1\}}\right) - \left(\overline{\theta}_{\mathrm{N_0}}^{\{0\}} + \sum_{n_0=1}^{N_0-1} \theta_{\mathrm{n_0}}^{\{0\}}\right)$. The number of parameters still remains $N_0 + N_1 - 3$.

4. Design Examples

In this section, we start with introducing the autocorrelation function (acf). Using the acf, we optimize some filter banks in terms of coding gain and show design examples, which have the first or second-order vanishing moments. In order to verify the significance of the vanishing moments, we compare frequency responses. Moreover, we confirm the symmetry from basis images. Through experiments, we compare the coding performance.

4.1 Autocorrelation Function (acf)

Let us define $x[\mathbf{n}]$ as a pixel value at a location $\mathbf{n}$, where $\mathbf{n}$ is a 2-D integer vector, $\mathbf{n} \in Z^2$. Then let us define a continuous vector $\mathbf{p} = (p_0, p_1)^T \in R^2$, and assume that pixel $x[\mathbf{n}]$ is sampled as $x(\mathbf{p})|_{\mathbf{p}=\mathbf{n}}$ from a 2-D continuous function $x(\mathbf{p})$.

A natural image $x(\mathbf{p})$ can often be modeled as a stational, zero-mean 2-D continuous-space random field $\tilde{x}(\mathbf{p})$ of which acf

$$R_{\tilde{x}\tilde{x}}(\boldsymbol{\tau}) = E\left[\tilde{x}(\mathbf{p}+\boldsymbol{\tau})\tilde{x}(\mathbf{p})\right] \tag{43}$$

doesn't depend on the location $\mathbf{p}$ but only distance $\boldsymbol{\tau} \in R^2$.

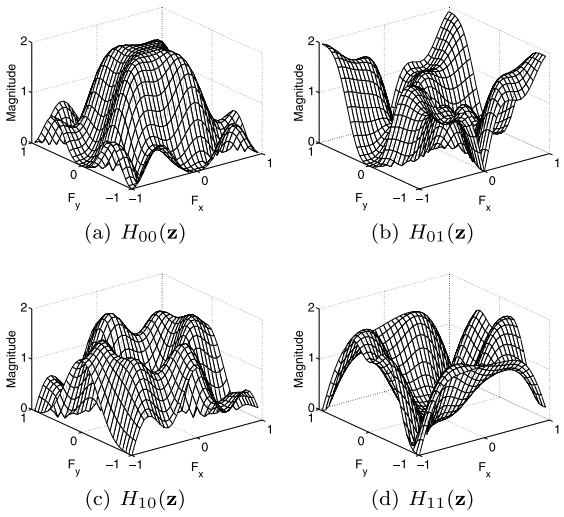

(a) $H_{00}(\mathbf{z})$ (b) $H_{01}(\mathbf{z})$ (c) $H_{10}(\mathbf{z})$ (d) $H_{11}(\mathbf{z})$

Fig. 3 Frequency responses of the minimal support filters with the 2nd-order vanishing moments of size 6×6 taps, $\rho_0 = \rho_1 = 0.95$.

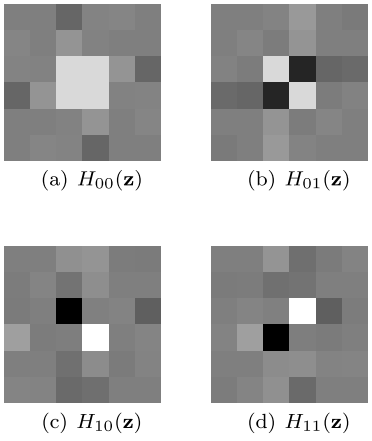

(a) $H_{00}(\mathbf{z})$ (b) $H_{01}(\mathbf{z})$ (c) $H_{10}(\mathbf{z})$ (d) $H_{11}(\mathbf{z})$

Fig. 4 Basis images of minimal support filters with the 2nd-order vanishing moments of size 6×6 taps, $\rho_0 = \rho_1 = 0.95$.

In our design examples of M-D filter banks, the following separable model is assumed:

$$R_{\tilde{x}\tilde{x}}(\boldsymbol{\tau}) = \rho_0^{|\tau_0|}\rho_1^{|\tau_1|}, \tag{44}$$

where $|\rho_0|, |\rho_1| < 1$ and τ_0 and τ_1 are elements of distance $\boldsymbol{\tau}$.

4.2 Design Examples and Coding Application

In the following design examples, the filter banks are optimized for maximizing coding gain, for the separable acf model in Eq. (44) with $\rho_0 = \rho_1 = 0.95$. We employed different optimization methods for the case of 1st-order and 2nd-order vanishing moments. For the 1st-order constraints or the 2nd-order case with $N_0, N_1 < 4$, we employed the unconstrained non-linear optimization function 'fminunc' in MATLAB R2008a. On the other hand, for the 2nd-order case with $N_0, N_1 > 3$, we employed the constrained non-linear optimization function 'fmincon' in MATLAB R2008a. For every case, the best result among several trials

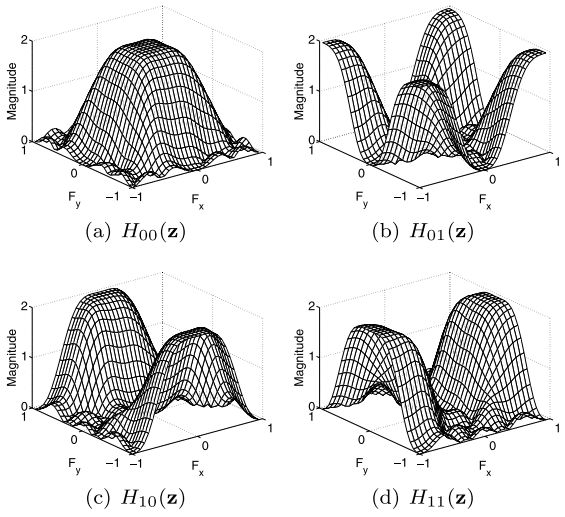

(a) $H_{00}(\mathbf{z})$ (b) $H_{01}(\mathbf{z})$

(c) $H_{10}(\mathbf{z})$ (d) $H_{11}(\mathbf{z})$

Fig. 5 Frequency responses of the designed filters with the 2nd-order vanishing moments of size 8×8 taps, $\rho_0 = \rho_1 = 0.95$.

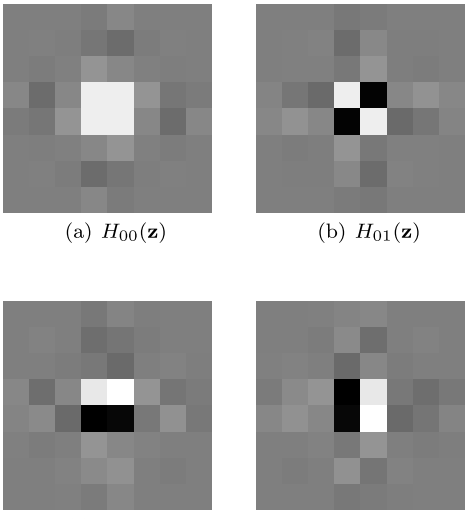

(a) $H_{00}(\mathbf{z})$ (b) $H_{01}(\mathbf{z})$

(c) $H_{10}(\mathbf{z})$ (d) $H_{11}(\mathbf{z})$

Fig. 6 Basis images of designed filters with the 2nd-order vanishing moments of size 8×8 taps, $\rho_0 = \rho_1 = 0.95$.

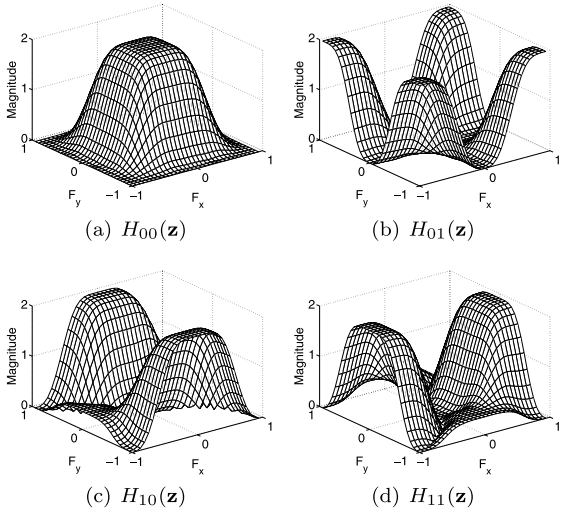

(a) $H_{00}(\mathbf{z})$ (b) $H_{01}(\mathbf{z})$

(c) $H_{10}(\mathbf{z})$ (d) $H_{11}(\mathbf{z})$

Fig. 7 Frequency responses of the designed filters with the 2nd-order vanishing moments of size 12×12 taps, $\rho_0 = \rho_1 = 0.95$.

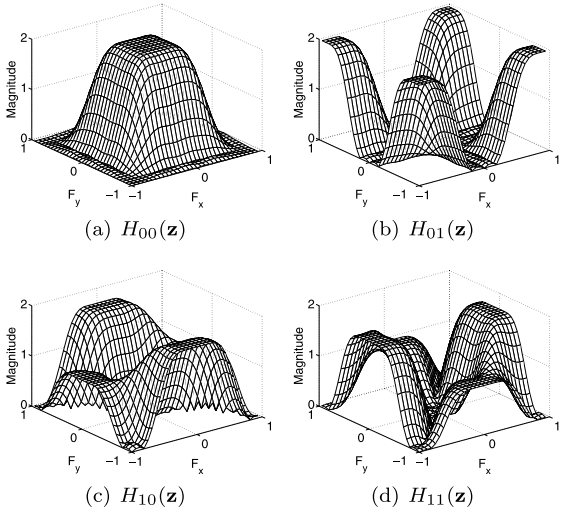

(a) $H_{00}(\mathbf{z})$ (b) $H_{01}(\mathbf{z})$

(c) $H_{10}(\mathbf{z})$ (d) $H_{11}(\mathbf{z})$

Fig. 8 Frequency responses of the designed filters with the 1st-order vanishing moments of size 12×12 taps, $\rho_0 = \rho_1 = 0.95$.

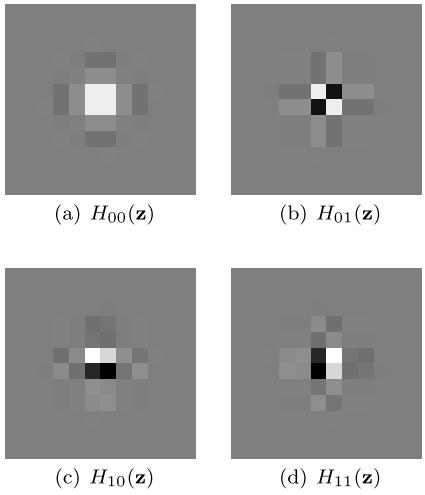

(a) $H_{00}(\mathbf{z})$ (b) $H_{01}(\mathbf{z})$

(c) $H_{10}(\mathbf{z})$ (d) $H_{11}(\mathbf{z})$

Fig. 9 Basis images of designed filters with the 2nd-order vanishing moments of size 12×12 taps, $\rho_0 = \rho_1 = 0.95$.

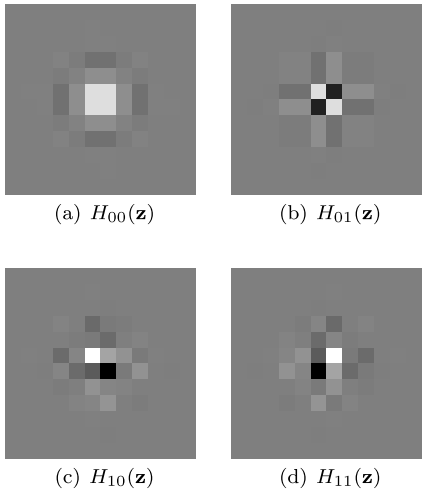

(a) $H_{00}(\mathbf{z})$ (b) $H_{01}(\mathbf{z})$

(c) $H_{10}(\mathbf{z})$ (d) $H_{11}(\mathbf{z})$

Fig. 10 Basis images of designed filters with the 1st-order vanishing moments of size 12×12 taps, $\rho_0 = \rho_1 = 0.95$.

of optimization process with randomly initialized parameters is selected to be shown.

Figures 3 and 4 are frequency responses and basis images of the minimal support design of size 6×6. As well, Figs. 5 and 6 show those of size 8×8.

Figure 7 shows the frequency responses of the resulting analysis filters of size 12×12 taps designed with the constraint of the second-order vanishing moments for $\rho_0 = \rho_1 = 0.95$, where the non-linear constraint functions $\|\mathbf{x}_3^{\{0\}}\| < 2$ and $\|\mathbf{x}_3^{\{1\}}\| < 2$ are used for the constrained optimization process.

$H_{00}(\mathbf{z})$ and $H_{01}(\mathbf{z})$ became a lowpass and highpass filter, respectively. From the paraunitary property, the impulse responses of the synthesis filters $F_{k\ell}(\mathbf{z})$ are given as the 180°-rotated version of these analysis filters $H_{k\ell}(\mathbf{z})$. Figure 8 shows an example with only the first-order vanishing moments of which size is 12×12 for $\rho_0 = \rho_1 = 0.95$. It is observed that the lowpass filter $H_{00}(\mathbf{z})$ shown in Fig. 7 is smoother than that in Fig. 8 at every aliasing frequency point as expected.

As well, we show basis images of designed filter banks. Figures 9 and 10 correspond to Figs. 7 and 8, respectively. It can be confirmed that the filter banks satisfy the symmetry.

The coding gains of filter banks are shown in the Ta-

Table 1 Coding gains of design examples.

	Vm1	Vm2			
	Coding Gain	σ_0	σ_1	flip	Coding Gain
NS DWT(6×6 taps)	10.18	0	1	off	8.44
NS DWT(8×8 taps)	10.72	1	1	on	10.06
NS DWT(10×10 taps)	11.57	0	1	on	11.45
NS DWT(12×12 taps)	11.60	0	0	on	11.52
NS DWT(14×14 taps)	11.65	1	0	on	11.60

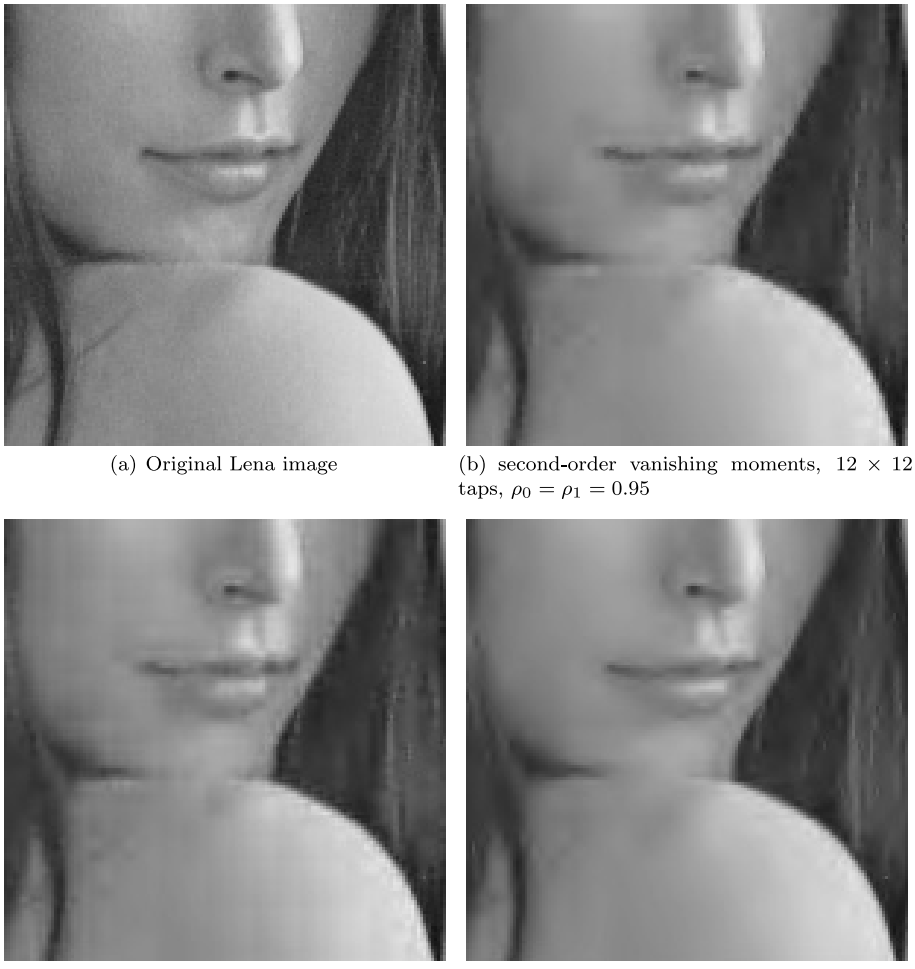

(a) Original Lena image

(b) second-order vanishing moments, 12×12 taps, $\rho_0 = \rho_1 = 0.95$

(c) first-order vanishing moments, 12×12 taps, $\rho_0 = \rho_1 = 0.95$

(d) 9/7DWT

Fig. 11 Experimental results of image coding (5-level DWT, 0.5[bpp]).

(a) Original Lena image

(b) second-order vanishing moments, 12×12 taps, $\rho_0 = \rho_1 = 0.95$

(c) first-order vanishing moments, 12×12 taps, $\rho_0 = \rho_1 = 0.95$

(d) 9/7DWT

Fig. 12 Experimental results of image coding (5-level DWT, 0.5[bpp]).

ble 1. For all design cases, the coding gain of filter banks with the 2nd-order vanishing moments shows lower value than that of the 1st-order one. It is natural because the constraints reduce the number of free parameters. Although the filters in Fig. 7 is imposed the second-order vanishing moments, the coding gain approaches to that of the filters only with the first-order vanishing moments.

4.3 Application to Image Coding

In order to verify the significance of the second-order vanishing moments, we show some results of image coding experiments.

In the experiments, we used five-level DWTs, and apply them to coding of Lena image (512×512, 8-bit, gray-scale) and Barbara image (320×240, 8-bit, gray-scale). In the transform domain, we applied the entropy coded scalar quantization (ECSQ) [1]. Figure 11 (a) shows part of the original Lena image. Reconstructed images are shown in Figs. 11 (b)(c) and (d), where subband quantization at average 0.5[bpp] is applied. Figures 11 (b) and (c) are obtained through 5-level DWTs with the filter banks corresponding to Figs. 7 and 8, respectively. For reference, the result of 9/7 DWT is shown in Fig. 11(d). Comparing Figs. 11(b) and (c), some structural artifacts are clearly noticed in (c), whereas they are suppressed in (b). The experimental results of Barbara image are shown in Fig. 12. As well as Lena in Fig. 11, the structural artifacts in (c) are suppressed in (b). PSNR results of our designed filter banks with the 5/3 and 9/7 DWT are summarized in Table 2. Almost all of results of the filter banks with the 2nd-order vanishing moments work better

Table 2 PSNR of reconstructed pictures with subband quantization at average 0.5[bpp], level 5.

Image	Lena		Barbara	
Vanishing Moment	Vm1	Vm2	Vm1	Vm2
NS DWT(6×6taps)	30.50	31.25	24.77	24.81
NS DWT(8×8taps)	31.53	31.98	25.38	25.76
NS DWT(10×10taps)	32.46	32.38	25.75	25.09
NS DWT(12×12taps)	32.31	32.52	25.44	25.86
NS DWT(14×14taps)	32.65	32.50	25.97	25.16
5/3 DWT	31.89		24.99	
9/7 DWT	33.12		26.22	

than 1st-order. The second-order vanishing moments make the smoothness of reconstructed images better. However, the performance of our designed filter banks is inferior to that of 9/7 DWT. We consider that our filter banks require more vanishing moments or directional characteristics.

5. Conclusions

In this paper, a design method of 2-D orthogonal symmetric wavelets was proposed by using a lattice structure for M-D LPPUFB, which the authors have proposed before and Lu Gan et al. have modified later. The derivation process of the constraints on the second-order vanishing moments was shown and some design examples obtained through optimization with the constraints were shown. By using the designed filter banks, we verified the significance through experimental results of image coding. In future, we will consider increasing the order of vanishing moments and investigate the filter directionality.

References

[1] D.S. Taubman and M.W. Marcellin, JPEG2000, Image Compression Fundamentals, Standards and Practice, Kluwer Academic Publishers, 2002.
[2] M. Ghanbari, "Standard codecs: Image compression to advanced video coding," The Institution of Electrical Engineers, 2003.
[3] I.E. Richardson, H.264 and MPEG-4 Video Compression, Wiley, 2003.
[4] P.P. Vaidyanathan, Multirate Systems and Filter Banks, Prentice Hall, 1993.
[5] J.W. Woods, Multidimensional Signal, Image and Video Processing and Coding, Academic Press, 2006.
[6] S. Muramatsu, A. Yamada, and H. Kiya, "A design method of multidimensional linear-phase paraunitary filter banks with a lattice structure," IEEE Trans. Signal Process., vol.47, no.3, pp.690–700, 1999.
[7] L. Gan and K.-K. Ma, "A simplified lattice factorization for linear-phase perfect reconstruction filter bank," IEEE Signal Process. Lett., vol.8, no.7, pp.207–209, 2001.
[8] D. Stanhill and Y.Y. Zeevi, "Two-dimensional orthogonal wavelets with vanishing moments," IEEE Trans. Signal Process., vol.44, no.10, pp.2579–2590, 1996.
[9] D. Stanhill and Y.Y. Zeevi, "Two-dimensional orthogonal filter banks and wavelets with linear phase," IEEE Trans. Signal Process., vol.46, no.1, pp.183–190, 1998.
[10] S. Oraintara, T.D. Tran, P.N. Heller, and T.Q. Nguen, "Lattice structure for regular paraunitary linear-phase filterbanks and m-band orthogonal symmetric wavelets," IEEE Trans. Signal Process., vol.49, no.11, pp.2659–2672, 2001.

Appendix A: Properties of Matrices in Sect. 3.3

The followings summarize some properties of matrices appeared in Sect. 3.3.

$$\mathbf{Q}(z^2)|_{z=\pm 1} = \mathbf{I}_4. \tag{A·1}$$

$$\frac{\partial}{\partial z}\mathbf{Q}(z^2) = z^{-3}\begin{pmatrix} -\mathbf{I}_2 & \mathbf{I}_2 \\ \mathbf{I}_2 & -\mathbf{I}_2 \end{pmatrix}. \tag{A·2}$$

$$\frac{\partial}{\partial z_0}\mathbf{d}(z_0, z_1) = \begin{pmatrix} 0 \\ -z_0^{-2} \\ 0 \\ -z_0^{-2}z_1^{-1} \end{pmatrix}. \tag{A·3}$$

$$\frac{\partial}{\partial z_1}\mathbf{d}(z_0, z_1) = \begin{pmatrix} 0 \\ 0 \\ -z_1^{-2} \\ -z_0^{-1}z_1^{-2} \end{pmatrix}. \tag{A·4}$$

Atsuyuki Adachi received B.E degree in electrical engineering from Niigata University in 2007. He is currently the candidate for the M.E. degree at Niigata University. His research interests are in digital signal processing, image/video processing, and video coding.

Shogo Muramatsu received B.E, M.E. and Ph.D. degrees in electrical engineering from Tokyo Metropolitan University in 1993, 1995 and 1998, respectively. From 1997 to 1999, he worked at Tokyo Metropolitan University. In 1999, he joined Niigata University, where he is currently an associate professor of Electrical and Electronics Engineering, Faculty of Engineering. During year from 2003 to 2004, he was a visiting researcher at University of Florence, Italy. His research interests are in digital signal processing, multi-rate systems, video analysis and hardware architecture. Dr. Muramatsu is a member of IEEE (Institute of Electrical and Electronics Engineers, Inc.), ITE (Institute of Image Information and Television Engineers), and IIEEJ (Institute of Image Electronics Engineers).

Hisakazu Kikuchi recieved B.E. and M.E. degrees from Niigata University, Niigata, Japan, in 1974 and 1976, respectively, and Dr.Eng. degree in electrical and electronic engineering from Tokyo Institute of Technology, Tokyo, Japan in 1988. From 1976 to 1979 he worked at Information Processing Systems Laboratory, Fujitsu, Ltd., Tokyo. Since 1979 he has been with Niigata University, where he is a Professor at Department of Electrical Engineering. During a year of 1992 to 1993, he was a visiting scientist at the California, Los Angeles. His research interests include digital signal processing, image/video processing, and wavelets as well as spread spectrum communication systems. Dr. Kikuchi is a member of IEEE (Institute of Electrical and Electronics Engineers), ITE (Institute of Image Information and Television Engineers of Japan), and Japan Society for Industrial and Applied Mathmematics, Research Institute of Signal Processing, and SPIE.